In Situ FTIR Studies on the Cold-Crystallization Process and Multiple Melting Behavior of Isotactic Polystyrene

Yongxin Duan,† Jianming Zhang,† Deyan Shen, and Shouke Yan*

State Key Laboratory of Polymer Physics & Chemistry, Joint Laboratory of Polymer Science and Materials, Institute of Chemistry, Chinese Academy of Sciences, Beijing 100080, P. R. China

Received January 4, 2003; Revised Manuscript Received April 28, 2003

ABSTRACT: The structure evolution of iPS during isothermal cold-crystallization and subsequent melting processes is studied by in situ monitoring its FTIR spectra. Through following the intensity changes of the characteristic bands associated with its crystalline status and 3_1 helix conformation chains, the multiple melting behavior of iPS cold-crystallized at different temperatures has been discussed in detail. It is concluded that (i) the lowest-temperature annealing peak can be ascribed either to the relaxing of locally ordered long 3_1 helix chains in the amorphous phase or to the melting of some microcrystallites formed upon long-time annealing; (ii) the double melting behavior of iPS cold-crystallized at temperatures lower than 180 °C is mainly attributed to the model of melting, recrystallization, and remelting of the iPS crystals; and (iii) for the sample cold-crystallized at a temperature of 200 °C, the in situ IR experiments give strong evidence to support the existence of different kinds of crystals which show different thermodynamic stabilities.

Introduction

The multiple melting behavior is not only a commonly encountered phenomenon of isothermally crystallized semicrystalline polymers but also a fundamentally important research subject for understanding the structure evolution of polymer during the heating process. Consequently, it has been one of the most extensively studied topics in the field of polymer science. In the past few decades, a substantial amount of work has been seen on the multiple melting behavior of different polymers.[1−11] Up to now, there exist obvious divergences concerning the origin of multiple melting behavior. This is not surprising for different polymer samples since their multiple melting behavior can be ascribed to some structure-dependent origins, such as different crystalline structures and modifications, multiple molecular weight distributions, and so on. This is, however, not expected for an individual polymer sample, e.g., isotactic polystyrene.

Isotactic polystyrene (iPS) is a semicrystalline polymer characterized by very slow crystallization rate and low crystallinity (about 30%). Its multiple melting behavior has been extensively investigated as an example of isotactic crystalline materials. Many techniques such as DSC,[5−7] X-ray,[8,9] and TEM[10,11] have been used to study its multiple melting behavior. However, there are still considerable controversies in the interpretation of each melting peak, especially for the lowest temperature endothermic peak (usually called the "annealing peak" for its position is always a few degrees above the annealing or crystallization temperature). On the basis of the DSC and TEM data, Lemstra et al.[6,7] suggested that the annealing peak originates from the melting of the secondary crystallized crystals trapped within the spherulites or intercrystalline links. They related the next (second) endothermic peak to the melting of the crystals generated through the normal primary crystallization process, while the last melting peak to the final melting of the crystals resulted from the melting and simultaneous recrystallization of the primary crystallized ones during the DSC scanning process. In the past few decades, the above-mentioned melting−recrystallization model for iPS was accepted by many authors. Strobl and Hussein[8,9] have demonstrated the recrystallization process of the cold-crystallized iPS samples according to their temperature-dependent SAXS measurements. Recently, Liu et al.[11] also investigated the multiple melting behavior of cold-crystallized iPS with DSC and TEM. They reported that (i) the "annealing peak" is not associated with the melting of subsidiary crystals formed by secondary crystallization as often suggested in the literature and (ii) two lamellar populations of different perfection within a single lamella are responsible for the so-called double melting behavior in iPS. Various analyses by many researchers have led to an in-depth understanding on the multiple melting behavior of iPS. However, a unique reasonable model for interpreting each melting peak of it is still not reached, and the relationship between molecular structural evolution and multiple melting behavior is still not seen. It is fair to state that a detailed structure analysis on a molecular level is necessary before a reasonable assignment of its multiple melting peaks can be made.

This study is motivated by a belief that new insight is helpful to clarify this issue further. FTIR, which is sensitive to both structural conformation and molecular environment, has become an important tool in characterizing semicrystalline polymers.[12] Detailed analyses are available on iPS regarding the band assignments. In situ monitoring changes of the crystalline, amorphous, and conformation sensitive bands during the heating process may shed more light on the multiple melting behavior of iPS, which is uncovered in the literature.

The purpose of this paper is to present some detailed FTIR experimental results and discussion regarding the origin of the multiple melting behavior of iPS. For a convenient comparison, some results of the DSC measurements are also included.

† Ph.D. candidates of the Chinese Academy of Sciences.

* To whom all correspondence should be addressed: Tel +86-10-8261 8476; Fax +86-10-6255 9373; e-mail skyan@iccas.ac.cn.

10.1021/ma034008f CCC: $25.00
Published on Web 06/03/2003

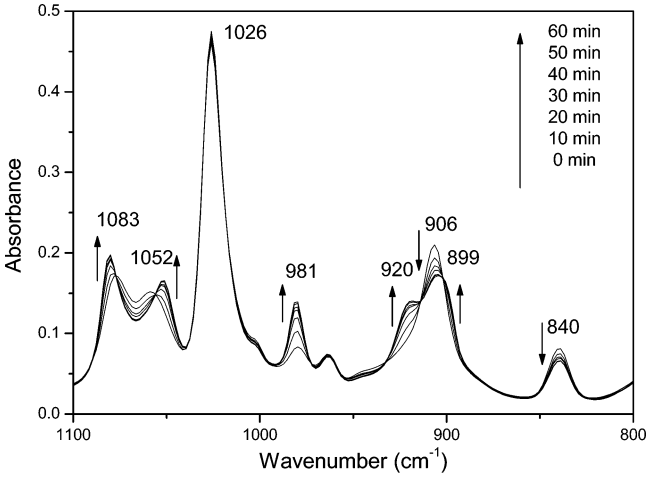

Figure 1. Temporal change of the IR spectrum in the wavenumber range of 800−1100 cm^{-1} during the cold-crystallization process of iPS at 160 °C. The spectra were recorded from 0 to 60 min with 10 min intervals.

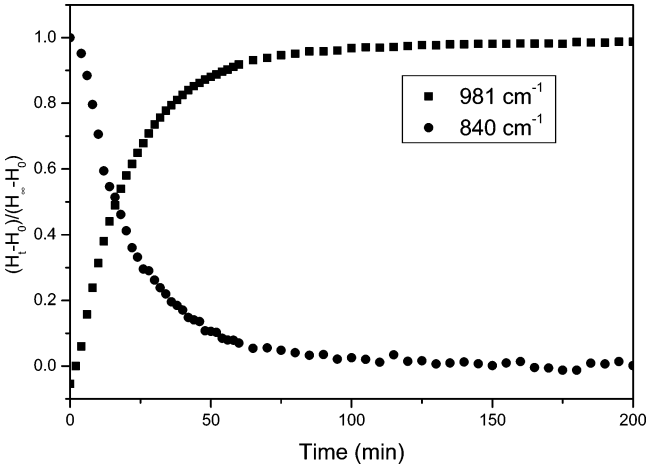

Figure 2. Peak heights of the crystalline band at 981 cm^{-1} and amorphous band at 840 cm^{-1} during the cold-crystallization at 160 °C as functions of crystallization time. Each peak height was normalized by the value at the longest crystallization time.

Experimental Section

The powder iPS sample (M_w = 400 000, with isotacticity of 90%) was purchased from Scientific Polymer Products, Inc. The amorphous thin films of about 10 μm in thickness were prepared by compression-molding the iPS powder at 250 °C with a pressure of 75 kg/cm^2 and subsequently quenched quickly into ice water at 0 °C. The dryness of the obtained amorphous thin films was carried out in a vacuum oven at room temperature for 24 h. To get cold-crystallized samples, the amorphous films were put between two round KBr plates with a spacer of polyimide (ca. 20 μm) and then annealed at various temperatures for different periods of time and subsequently quenched to room temperature on air. It was demonstrated that the room temperature quenching stops the iPS crystallization process from both melt and glassy states immediately.

The thus-prepared specimen was set on a Bruker P/N 21525 series variable temperature cell, which was placed in the sample compartment of a Bruker EQUINOX 55 spectrometer equipped with a DTGS detector. FTIR spectra of the specimens were in situ recorded at 2 °C intervals with a heating rate of 2 °C/min from 40 to 250 °C. The spectra were obtained by averaging 32 scans at a 4 cm^{-1} resolution, which took about 30 s. It was difficult to calculate the integrated intensity precisely since some peaks overlapped heavily. Therefore, peak height was chosen for data analysis. To different peak shape, a suitable method for calculating the peak height and drawing the baseline was chosen from the Bruker OPUS software.

DSC measurements of the cold-crystallized iPS samples were carried out on a Mettler Toledo-822e differential scanning calorimeter with ca. 5 mg iPS samples sealed in aluminum pans. Nitrogen gas purge with a flux of ca. 50 mL/min was used to prevent oxidative degradation of the samples during heating runs. The rate of the heating run in DSC was also 2 °C/min in order to conduct a reasonable comparison with the FTIR results.

Results

FTIR Study on Cold-Crystallization Processes. The isothermal cold-crystallization processes of iPS at different crystallization temperatures were in situ monitored by FTIR. The infrared spectra of iPS recorded during isothermal cold-crystallization process of iPS at 160 °C for a variety of times are shown in Figure 1. The band assignments given in the literature are used for the structure analyses.[13−16] It was well documented that the band at 981 cm^{-1} is a crystallization-sensitive band with an intensity increment in proportion to the degree of crystallinity. The bands located at 899, 920, 1052, and 1083 cm^{-1} are generated by the 3_1 helix chains, while the bands located at 840 and 906 cm^{-1} are associated with its amorphous phase. The appearances of the 3_1 helix bands depend on the sequence length of the helix unit. Kobayashi and co-workers[15,17] have introduced a concept of critical sequence length, which depicts the shortest length of the regular sequence with particular conformation necessary for the appearance of some 3_1 helix band. The critical sequence lengths for 3_1 helix bands in the spectrum are different from band to band, e.g. 16 for 899 cm^{-1}, 10 for 920 and 1052 cm^{-1}, and 5 for 1083 cm^{-1}. The splitting of the 1052 and 1083 cm^{-1} bands is mainly related to the regularity of the skeletal chain. The band at 1026 cm^{-1} is due to the localized vibrational mode associated with C−H in-plane bending of the phenyl ring. This band is usually chosen as an internal standard since it is not affected by its crystalline status.[18] From Figure 1, it can be clearly seen that the intensities of the bands associated with the crystalline and 3_1 helix chains of iPS located at 981, 899, 920, 1052, and 1083 cm^{-1} increase with time, while those associated with its amorphous counterpart at 840 and 906 cm^{-1} decrease with time. This unambiguously indicates the progress of crystallization process. The band at 981 cm^{-1} is used here to characterize the cold-crystallization and melting processes of iPS due to the direct correlation between its intensity and the degree of crystallinity. For clarity, an intensity change ratio is defined as $(H_t - H_0)/(H_\infty - H_0)$, where H_0, H_t, and H_∞ represent the peak height of the original sample, crystallized for a time "t" and after completion of the crystallization, respectively. The intensity change ratio as a function of crystallization time is plotted in Figure 2. For a clear comparison, the intensity change ratio of the amorphous band at 840 cm^{-1} is also included. It is clear that the intensity of the crystalline band at 981 cm^{-1} increases with the increase of the crystallization time very rapidly for the first hour and henceforth slows down gradually with the further increase of the crystallization time. On the contrary, the intensity decrease of the amorphous band at 840 cm^{-1} is synchronized with the increase in the crystal band at 981 cm^{-1}. The intensity change ratio vs time plots of both bands at 981 and 840 cm^{-1} turn almost flat after being annealed at 160 °C for 2 h. From this result, it is fair to state that the cold-crystallization of iPS at 160 °C is basically

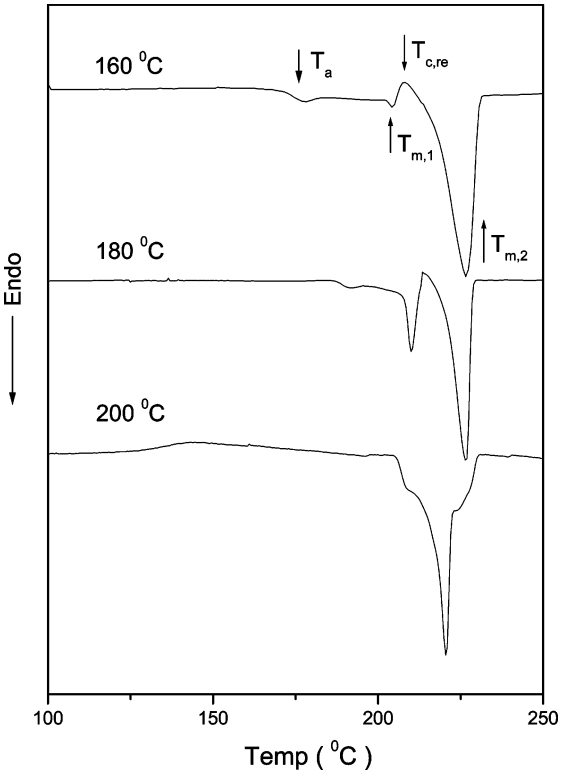

Figure 3. DSC heating curves of iPS cold-crystallized isothermally respectively at 160, 180, and 200 °C for 6 h.

completed in the first 2 h. Similar results are obtained for the samples cold-crystallized isothermally at 180 and 200 °C.

DSC Measurements on the Melting Processes. DSC measurements were performed on the samples cold-crystallized isothermally at 160, 180, and 200 °C for 6 h. The heating rates of all DSC runs were 2 °C/min for a reasonable comparison with the FTIR results represented in the next paragraph. As shown in Figure 3, the following can be identified: (i) There exhibit obviously three endothermic peaks as labeled T_a, $T_{m,1}$, and $T_{m,2}$ (in the order of temperature from low to high). (ii) The lowest-temperature endotherm, i.e., the so-called annealing peak (T_a), shifts to higher temperatures with increasing crystallization temperature. It appears always at ca. 10−15 °C above the crystallization temperature. It merges into the $T_{m,1}$ (the lowest-temperature melting peak) as a shoulder when the sample was crystallized at 200 °C for 6 h. (iii) The $T_{m,1}$ shifts also to higher temperatures with increasing crystallization temperature. It merges finally into the $T_{m,2}$ and results in the $T_{m,2}$ appearing as a shoulder of it. Moreover, the peak height of $T_{m,1}$ is evidently enhanced with increasing T_c. (iv) Even though the $T_{m,2}$ peak size decreases gradually with the increase of T_c, its temperature remains almost constant around 225 °C. (v) An exothermic recrystallization peak (labeled as $T_{c,re}$), which is located between the last two melting peaks, can be recognized for the samples crystallized at 160 and 180 °C. All of the aforementioned features demonstrate the remarkable dependence of the multiple melting peaks on the crystallization condition.

In Situ FTIR Study on the Melting Processes. To study the melting processes of the cold-crystallized iPS samples on a molecular level by the IR technique, IR spectrum of the iPS samples cold-crystallized at different temperatures were in situ recorded during the heating processes at 2 °C temperature intervals, and the intensity changes of the characteristic peaks were followed. The samples were heated from 40 to 250 °C with a rate of 2 °C/min, the same as used in the DSC measurements. All of the data are normalized with the internal band at 1026 cm^{-1}. Figure 4 shows the peak height changes of the amorphous band at 840 cm^{-1} and crystalline band at 981 cm^{-1} in the sample cold-crystallized at 160 °C for 6 h. Mainly two features of Figure 4 should be addressed. First of all, there are conspicuous transitions of both bands in the temperature range from 170 to 178 °C. In this temperature region, the intensity of crystalline band decreases more quickly accompanied by the intensity rapid increase of amorphous band. Second, beginning at 212 °C, an intensity increase of the crystalline band at 981 cm^{-1} and meanwhile an intensity decrease of the amorphous band at 840 cm^{-1} are identified with the elevation of the temperature. While the intensity of the crystalline band at 981 cm^{-1} reaches a maximum value at 225 °C, the intensity of the amorphous band at 840 cm^{-1} falls to its minimum position again. Hereafter, steep intensity decrease of the crystalline band at 981 cm^{-1} and increase of the amorphous band at 840 cm^{-1} are observed. This undoubtedly illustrates the crystallinity changes of the sample during heating process. With increment of the temperature, the peak height change of the 3_1 helix band at 920 cm^{-1} reveals a similar disciplinarian as that of the crystalline band at 981 cm^{-1}. As shown in Figure 5, in the temperature range from 100 to 160 °C, the peak height of this band decreases gradually as the temperature increases. This kind of change, as can also be recognized in Figure 4 for the crystalline band at 981 cm^{-1}, is attributed to a temperature effect. Normally, a gradually decrease of the IR peak intensities caused by changes of intermolecular interactions can be observed as the temperature increases.[19] In the temperature range 170−178 °C, the peak height of the 3_1 helix band at 920 cm^{-1} exhibits also a steep decrease. At about 210 °C, a further tiny stepwise decrease of its intensity followed by a rapid increase from 212 °C up to 230 °C is seen. The peak intensity declines finally at about 230 °C and reaches its minimum value at about 250 °C.

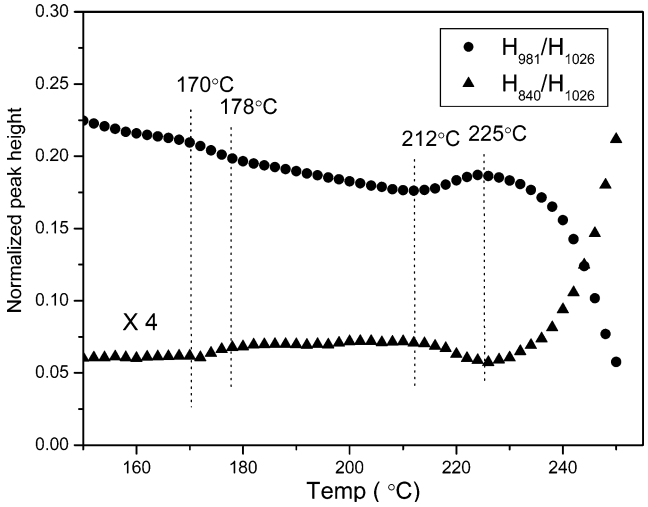

Figure 4. Changes in the peak height of the crystalline band at 981 cm^{-1} and amorphous band at 840 cm^{-1} with the elevation of temperature during the heating process. The heating rate is 2 °C /min, and the iPS sample was cold-crystallized at 160 °C for 6 h.

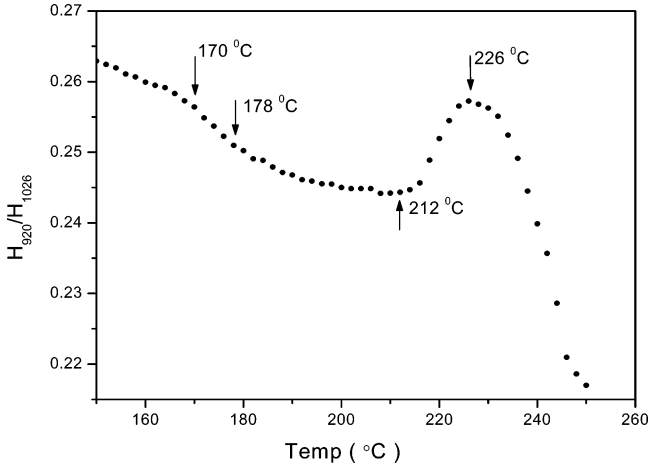

Figure 5. Change in the peak height of the 3_1 helix band at 920 cm^{-1} of the iPS sample cold-crystallized at 160 °C for 6 h during heating process. The heating rate is 2 °C /min.

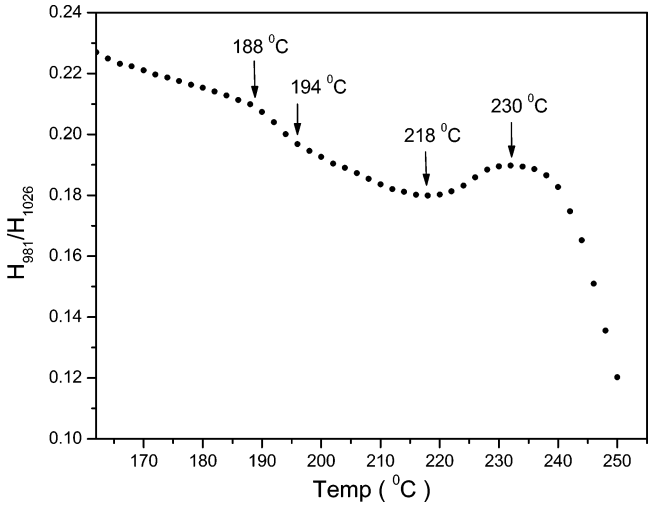

Figure 6. Change in the peak height of the crystalline band at 981 cm^{-1} of the iPS sample cold-crystallized at 180 °C for 6 h during heating. The heating rate is the same as in Figure 5.

Similar results were obtained for the samples cold-crystallized at 180 °C for 6 h. Figure 6 shows its peak height change of the crystalline band at 981 cm^{-1} as a function of temperature during heating. The heating rate was also 2 °C/min. The only difference of Figure 6 with respect to Figure 4 is that the temperature range for the first abrupt intensity change is now shifted to 190−195 °C, while the temperature for the occurrence of the rapid intensity increase is shifted to ca. 220 °C.

If the samples were isothermally crystallized at 200 °C for 6 h, the intensity change of the crystalline band at 981 cm^{-1} with temperature is somewhat different from those crystallized at 160 and 180 °C. As shown in Figure 7, there occur two apparent stepwise intensity reductions at temperatures of 210 and 230 °C. The inset illustrates its change rate with temperature. No evident intensity increase can be identified in the whole heating process.

Discussion

According to the above results, the origin of the multiple melting behavior of the cold-crystallized iPS samples can be discussed. First of all, during the heating course, there are significant peak height changes of the crystalline band at 981 cm^{-1}, the amorphous band at

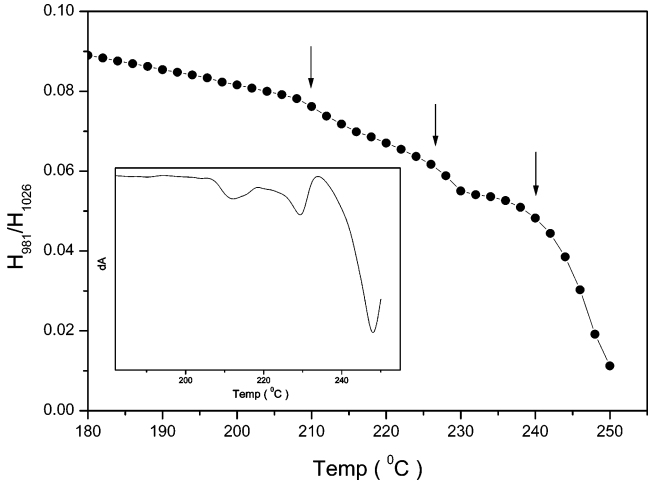

Figure 7. Change in the peak height of the crystalline band at 981 cm^{-1} of the iPS sample cold-crystallized at 200 °C for 6 h during heating. The inserted graph shows the change rate of peak height with temperature.

840 cm^{-1}, and the 3_1 helix band at 920 cm^{-1}. This unambiguously indicates the crystallinity and crystalline structure changes of the sample during heating. Comparing the IR results with those of the DSC measurements, it is reasonable to assign the first (the lowest temperature) stepwise changes of peak intensity for each sample to the so-called "annealing peak" appeared in the DSC curves. As concluded from the DSC results, the temperature ranges for the first intensity change shift also to higher temperatures with elevation of crystallization temperature but appear always at ca. 10 °C above the cold-crystallization temperatures. As for the origin of this peak, there exist many different explanations. Lemstra and co-workers suggested that the annealing peak originates from the melting of the secondary crystallized crystals trapped within the spherulites or intercrystalline links, e.g., tie molecules.[6,7] Mohame et al. also believed that the annealing peak is associated with melting of small crystallites coupled to the mobilization of a rigid amorphous third phase.[20] Through morphological studies of the samples cold-crystallized at 160 °C for 12 h and subsequently heat-treated at variety of conditions, Petermann et al.[21,22] found that there is no evident difference in the lamellar morphology before and after thermal treatment. Therefore, they claimed that this small endotherm (T_a) does not originate from the melting of secondary crystals. They related this peak to the enthalpy relaxation of a pseudo-crystalline interphase between the amorphous and crystalline phases. In our in situ FTIR experiments, apparent intensity changes of the bands associated with its crystalline status have been recognized. Since the intensity changes of crystalline and amorphous bands can be directly related to the change of its crystallinity, the above obtained result clearly indicates that a small amount of crystals have melted in this temperature range. Unfortunately, these molten crystallites have not been recognized in the TEM observation. Considering that the TEM experiments are not an in situ procedure, some tiny morphological changes on the bright field electron micrographs could be overlooked.

Combining the above-mentioned results with the explanations presented in the literature, it can be concluded that the annealing peak may originate from the melting of either the subsidiary crystals as proposed by Lemstra et al.[6,7] and Mohame et al.[20] or the pseudo-

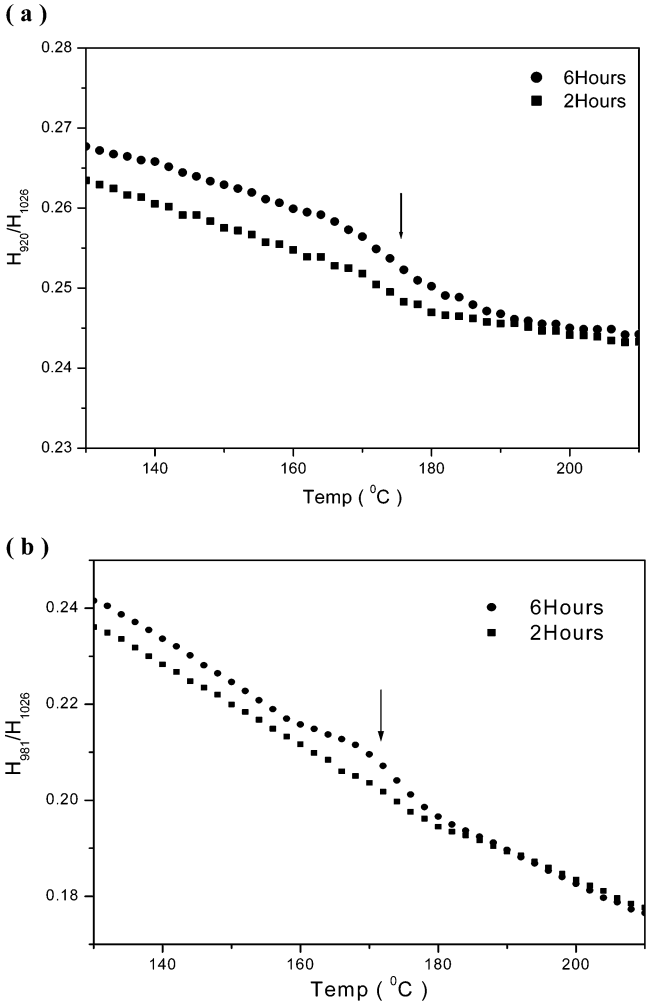

Figure 8. Changes in the peak height of the crystalline band at 981 cm^{-1} (a) and the 3_1 helix band at 920 cm^{-1} (b) during the heating process. The iPS samples were cold-crystallized at 160 °C for 2 h (designated by symbol ■) and 6 h (designated by symbol ●). The heating rate is 2 °C/min.

crystalline interphase between the amorphous and crystalline phases as mentioned by Petermann et al.[21,22] To get a detailed insight into these molten crystallites, the FTIR experiments were focused on the temperature range in which the annealing peak appears, e.g., 130−200 °C. Parts a and b of Figure 8 illustrate the intensity changes of the 981 cm^{-1} crystalline band and 920 cm^{-1} 3_1 helix band of the iPS samples crystallized at 160 °C for 2 and 6 h, respectively. From Figure 8a, it is clear that no intensity transition of the crystalline band at 981 cm^{-1} at the temperature of annealing peak can be identified with the sample cold-crystallized for 2 h at 160 °C. This is quite different from the DSC measurements which show apparent annealing peaks with all of the samples cold-crystallized at 160 °C for more than 40 min.[10] For the 3_1 helix band at 920 cm^{-1}, however, there are clearly intensity transitions of both samples at the temperature of annealing peak (see Figure 8b). Taking into account that the appearance of the 920 cm^{-1} band in the spectrum is related to a kind of 3_1 helix sequence (the critical sequence length of it is 10), the above-obtained results may imply that, in DSC curves, the annealing peak appearing in the sample cold-crystallized at 160 °C for 2 h resulted from the relaxing of locally ordered long 3_1 helix chains in the amorphous phase rather than the melting of any kind of crystallites. With increasing crystallization time, e.g., crystallized at 160 °C for 6 h, the locally ordered long 3_1 helix chains may aggregate and form small crystallites. If this hypothesis holds true, then the annealing peak of the samples cold-crystallized at 160 °C for 6 h can be ascribed to the melting of these microcrystallites.

Furthermore, from Figures 4 and 6, it can be clearly seen that the intensities of the crystalline band at 981 cm^{-1} in the samples cold-crystallized for 6 h at 160 and 180 °C begin to increase again at the temperatures of 212 and 220 °C, respectively. This intensity increase is concomitant with the intensity decrease of the amorphous band at 840 cm^{-1} and indicates an increase of the crystallinity of the sample. This demonstrates conspicuously the occurrence of a recrystallization process during the heating experiments. This result is in consistent with that of other experiments,[10,23,24] which also indicate a recrystallization process at high temperature during heating. The subsequent intensity rapid decrease of both the crystalline and 3_1 helix bands describes unambiguously the final melting of the recrystallized crystals. Of course, this cannot exclude the existence of some crystals formed by normal primary crystallization but with higher thermodynamic stability. This result leads to the conclusion that the highest-temperature melting peak of the samples cold-crystallized at temperatures lower than 180 °C may be mainly contributed by the melting of the crystals produced during the course of melt recrystallization at $T_{m,1}$.

It should be pointed out that the first melting peak, indicated as $T_{m,1}$ on the DSC curves, has not been revealed by the FTIR study. This may be explained as that the melting of the materials at $T_{m,1}$ is followed by instantaneous recrystallization. The recrystallization rate of these molten materials may be too fast to be resolved by the experimental procedure as used here. As a consequence, only resulted total increase of crystallinity has been illustrated by the IR measurement.

Finally, the FTIR result on the melting process of the iPS sample cold-crystallized isothermally at 200 °C for 6 h indicates that the peak intensity of the crystalline band at 981 cm^{-1} decreases continuously with three distinct transitions (see Figure 7). These transitions can be assigned to the three melting peaks observed in the DSC curves. This clearly indicates that the $T_{m,1}$ and $T_{m,2}$ of the samples cold-crystallized at 200 °C are caused by melting of crystals with different perfection. Moreover, in agreement with the DSC results, the recrystallization process has been inhibited by annealing the sample at higher temperature, e.g., 200 °C.

Conclusions

The structure evolution of iPS during isothermal cold-crystallization and subsequent melting processes are studied by in situ monitoring its FTIR spectra. Through following the intensity changes of the crystalline band at 981 cm^{-1}, the amorphous band at 840 cm^{-1}, and the 3_1 helix conformation band at 920 cm^{-1}, the FTIR has for the first time been used to study the multiple melting behavior of the iPS cold-crystallized at different temperatures. According to the obtained FTIR data, it can be concluded that (i) the lowest-temperature annealing peak can be ascribed either to the relaxing of locally ordered long 3_1 helix chains in the amorphous phase or to the melting of some microcrystallites formed upon long-time annealing; (ii) the double melting behavior of iPS cold-crystallized at temperatures lower than 180 °C

is mainly attributed to the melting of iPS crystals produced during the course of the melt recrystallization at $T_{m,1}$; and (iii) for the sample cold-crystallized at temperature of 200 °C, the in situ IR experiments give strong evidence to support the existence of different kinds of crystals which show different thermodynamic stabilities.

Acknowledgment. The financial support of the National Natural Science Foundation of China (No. 20244003) and the CAS hundred talents program are gratefully acknowledged.

References and Notes

(1) Huang, B. S.; Chang, L. L.; Woo, E. M. *Colloid Polym. Sci.* **2001**, *279*, 887.
(2) Denchev, Z.; Nogales, A.; Ezquerra, T. A.; Fernandes-Nascimento, J.; Baltà-Calleja, F. J. *J. Polym. Sci., Part B*: *Polym. Phys.* **2000**, *38*, 1167.
(3) Zhou, W.; Cheng, S. Z. D.; Putthanarat, S.; Eby, R. K.; Reneker, D. H.; Lotz, B.; Magonov, S.; Hsieh, E. T.; Geerts, R. G.; Palackal, S. J.; Hawley, G. R.; Welch, M. B. *Macromolecules* **2000**, *33*, 6861.
(4) Alizadeh, A.; Richardson, L.; Xu, J.; McCartney, S.; Marand, H.; Cheung, Y. W.; Chum, S. *Macromolecules* **1999**, *32*, 6221.
(5) Boon, J.; Challa, G.; Krevelen, D. V. *J. Polym. Sci.* **1968**, *6*, 1791.
(6) Lemstra, P. J.; Kooistra, T.; Challa, G. *J. Polym. Sci.* **1972**, *10*, 823.
(7) Lemstra, P. J.; Schouten, A. J.; Challa, G. *J. Polym. Sci., Polym. Phys. Ed.* **1974**, *12*, 1565.
(8) Hussein, M. A.; Strobl, G. *Eur. Phys. J. E.* **2001**, *6*, 305.
(9) Hussein, M. A.; Strobl, G. *Macromolecules* **2002**, *35*, 1672.
(10) Liu, T. X.; Petermann, J. *Polymer* **2001**, *42*, 6453.
(11) Liu, T. X.; Petermann, J.; He, C. B.; Liu, Z. H.; Chung, T. S. *Macromolecules* **2001**, *34*, 4305.
(12) Esposito, L. D.; Koenig, J. L. *J. Polym. Sci., Polym. Phys. Ed.* **1976**, *12*, 1731.
(13) Kobayashi, M.; Tsumura, K.; Tadokoro, H. *J. Polym. Sci.* **1968**, *6*, 1493.
(14) Painter, P. C.; Koenig, J. L. *J. Polym. Sci., Part B*: *Polym. Phys.* **1982**, *2*, 2277.
(15) Kobayashi, M.; Nakaoki, T.; Ishihara, N. *Macromolecules* **1990**, *23*, 78.
(16) Nakaoki, T.; Katagiri, C.; Kobayashi, M. *Macromolecules* **2002**, *35*, 7708.
(17) Kobayashi, M.; Akita, K.; Tadokoro, H. *Makromol. Chem.* **1968**, *118*, 324.
(18) Kimura, T.; Ezure, H.; Tanaka, S.; Ito, E. *J. Polym. Sci., Part B*: *Polym. Phys.* **1998**, *36*, 1227.
(19) O'Reill, J. M.; Mosher, R. A. *Macromolecules* **1981**, *14*, 602.
(20) Schick, C.; Wurm, A.; Mohamed, A. *Colloid Polym. Sci.* **2001**, *279*, 800.
(21) Bonnet, M.; Rogausch, K.-D.; Petermann, J. *Colloid Polym. Sci.* **1999**, *277*, 513.
(22) Liu, T.; Yan, S.; Bonnet, M.; Liberwirth, I.; Rogausch, K.-D.; Petermann, J. *J. Mater. Sci.* **2000**, *35*, 5047.
(23) Rim, P. B.; Runt, J. P. *Macromolecules* **1984**, *17*, 1520.
(24) Plans, J.; Macknight, W. J.; Karasz, F. E. *Macromolecules* **1984**, *17*, 810.

MA034008F